buildings

MDPI

Review

Challenges in Daytime Outdoor Glare Evaluation Within the Built Environment: A Review

Ying He [1,2], Huan Yu [1], Yuan Chen [1], Ayin Yan [1], Yuli Wang [1] and Jingfeng Xu [1,2,*]

[1] Faculty of Architecture and Urban Planning, Chongqing University, Chongqing 400045, China; he_ying@cqu.edu.cn (Y.H.); 20194431@cqu.edu.cn (H.Y.); 20241501008@stu.cqu.edu.cn (Y.C.); 20241501002@stu.cqu.edu.cn (A.Y.); 202415021003@stu.cqu.edu.cn (Y.W.)
[2] Key Laboratory of New Technology for Construction of Cities in Mountain Area, Chongqing 400045, China
* Correspondence: xujingfeng@cqu.edu.cn

Abstract

Direct sunlight and reflections from buildings and ground surfaces create multi-source highlights in high-density built environments, potentially affecting outdoor visual safety and spatial use. This integrative review synthesizes daytime outdoor glare research in terms of physical characteristics, observer effects, and assessment methods. Solar movement, surface reflection, spatial obstruction, and observer movement jointly alter the intensity, direction, scale, and number of bright regions. Outdoor glare is therefore high-luminance, multi-source, non-uniform, and time-varying, occurring as concentrated, continuous-area, and discrete-patch highlights. Evidence indicates that outdoor glare causes visual discomfort, impairs target recognition, and may induce immediate behavioral adjustments. However, studies focus mainly on static viewpoints, short-term perception, and driving tasks, with limited direct observation of spatial-use outcomes such as dwell time, detouring, and location choice. Current assessments identify potential exposure through geometric-path analysis or quantify glare stimuli using established indices and extended models. Some metrics support relative comparisons within specific settings but cannot simultaneously characterize spatial reachability, stimulus intensity, dynamic exposure, and observer responses. Future research should develop hierarchical, type-specific dynamic assessment methods based on glare source, spatial scale, and visual task to inform building-envelope design, material selection, and outdoor glare-risk control.

Keywords: daylight glare; outdoor glare; glare assessment; high-luminance sources; built environment

Check for updates

Academic Editor: Chi-Ming Lai

Received: 20 September 2026
Revised: 14 October 2026
Accepted: 18 October 2026
Published: 23 October 2026

Copyright: © 2026 by the authors. Licensee MDPI, Basel, Switzerland. This article is an open access article distributed under the terms and conditions of the Creative Commons Attribution (CC BY) license.

1. Introduction

As the built environment continues to evolve, high-density development and mixed-use functions have become defining characteristics of the spaces in which people conduct their daily activities [1]. The intensification of spatial form, together with continuing advances in building materials and construction technologies, has substantially altered the luminance structure and spatial distribution of daytime outdoor light environments [2]. Increases in building height and massing, combined with narrower street spaces, make direct sunlight and its reflections from building and ground surfaces more likely to enter the fields of view of pedestrians and drivers [3]. Meanwhile, the widespread use of highly reflective glass curtain walls [4], metal façades [5,6], new paving materials, and photovoltaic installations has further increased the number and spatial extent of potential intense reflection sources in built environments.

In built environments, direct sunlight is a high-intensity natural light stimulus that persists throughout the daytime outdoor environment [7] and coexists spatially with bright reflected regions produced by highly reflective built surfaces. Consequently, daytime outdoor light stimuli are characterized by high luminance levels, diverse sources, and pronounced directionality, and glare is widely distributed across urban roads, public spaces, and pedestrian environments. Solar trajectories, street orientation, and building obstructions can also cause bright stimuli to recur at specific locations and times, resulting in marked spatiotemporal specificity [2,3].

In daytime outdoor built environments, glare generally refers to interference with visual function or visual comfort caused by bright stimuli within the field of view and is commonly classified as disability glare or discomfort glare [7]. Previous studies have shown that direct sunlight and building reflections can cause subjective discomfort ranging from perceptible to disturbing and can also impair target recognition and environmental judgment [8,9], thereby affecting urban traffic safety [10] and visual comfort in public spaces [11].

Compared with indoor or nighttime lighting conditions, the causes and manifestations of daytime outdoor glare are more complex. Bright stimuli may originate from direct sunlight at low solar altitudes or from specular and semi-specular reflections produced by building façades, pavements, water surfaces, and other interfaces. Under natural-light conditions, the intensity and direction of bright stimuli change continuously with solar position, spatial obstructions, and observer movement [12]. Urban outdoor spaces also accommodate driving, walking, and public interaction, requiring individuals to perceive their surroundings and make decisions while moving continuously [13]. Crash statistics and retrospective studies have identified an association between daytime solar glare and the risk of fatal pedestrian injury [14]. Under low-solar-altitude conditions in the morning and evening, approximately 40% of urban roads may be exposed to solar glare during specific periods, while the associated crash risk varies with road orientation and obstruction conditions [15].

Although glare research has established a relatively mature theoretical foundation and assessment system [16], systematic assessment methods specifically developed for daytime outdoor settings in built environments remain inadequate [17]. Recent studies have further identified limitations in existing assessment criteria, perceptual validation, and cross-context applicability [18,19]. These limitations restrict the effective quantification and management of complex outdoor-glare risks and hinder the development of evidence-based strategies for urban design and safety management.

Accordingly, this study adopts an integrative review approach to systematically examine research on glare in daytime outdoor built environments, focusing on three questions: What are the luminance characteristics, spatial geometry, and forms of daytime outdoor glare? How does glare exposure affect observers' subjective perception, visual function, and spatial behavior? What aspects can existing geometric-path and glare-index methods assess, and what are their boundaries of applicability? This review aims to connect the physical characteristics of glare, its effects on observers, and available assessment methods; clarify the scope and limitations of the existing evidence; and provide a research foundation for assessing glare risks associated with building form, reflective materials, and outdoor spaces.

2. Methodology

Because relatively few studies have directly focused on the assessment of daytime outdoor glare in built environments, and most have discussed direct or reflected glare separately, the available literature is highly heterogeneous in terms of scenario configura-

tion, task constraints, metric systems, and data-acquisition methods. This heterogeneity makes standardized effect-size extraction and statistical synthesis difficult. Given these characteristics, this study adopted an integrative review approach [20] to synthesize the physical characteristics, observer effects, and assessment methods of daytime outdoor glare and to examine the relationships among different research approaches and their boundaries of applicability.

The literature search focused on the environmental characteristics, observer effects, and assessment methods of daytime outdoor glare. Search terms covered glare types, application settings, physical parameters, and assessment techniques, including "glare", "daytime glare", "outdoor glare", "solar glare", "reflected glare", "discomfort glare", "disability glare", "glare evaluation", "luminance", "contrast", "veiling luminance", "HDR imaging", and "luminance mapping". These terms were combined using Boolean operators with scenario-related terms and their synonyms concerning building façades, roads, public spaces, pedestrians, and driving. The databases searched were the Web of Science Core Collection and Google Scholar, with coverage extending through September 2026. To identify studies potentially missed by the interdisciplinary search, backward reference searching and forward citation tracking were also conducted for the included studies and relevant reviews. The evidence synthesis primarily included peer-reviewed journal articles published in English. Conference papers were retained when they provided complete descriptions of research methods, scenario conditions, or measured data. A limited number of standards, monographs, dissertations, and technical reports were additionally included to clarify glare definitions, the origins of assessment metrics, and standard requirements; however, they were not treated as primary evidence of the effects of outdoor glare.

Following the initial search, titles and abstracts were first screened for relevance, and studies clearly unrelated to the review topic were excluded. Full texts were then examined and reassessed according to the study object, glare-source type, research setting, assessment metrics, and principal findings. Full-text screening involved three authors with relevant research backgrounds. Disagreements between the primary reviewers were resolved through discussion and, when necessary, adjudication by the third author.

According to the literature-selection criteria established for this review, the following types of studies were excluded:

- Studies focusing solely on glare under indoor lighting conditions or in nighttime lighting scenarios;
- Daylighting-performance studies that did not treat glare perception or glare evaluation as a central research question;
- Studies focusing primarily on light pollution or macro-scale impacts of the light environment, such as ecological effects and night-sky brightness;
- Studies discussing only the optical properties or reflectance parameters of materials without addressing glare exposure, visual responses, or glare-evaluation metrics.

The remainder of this paper is organized as follows. Section 3 examines the luminance characteristics, spatial geometry, and forms of daytime outdoor glare. Section 4 analyzes its effects on visual function, perceived discomfort, and spatial behavior. Section 5 reviews assessment methods based on geometric paths and mathematical models. Section 6 discusses the limitations of existing research, design applications, and future research directions and summarizes the main conclusions.

3. Characteristics of Daytime Outdoor Glare

3.1. Luminance of Outdoor Glare

Daytime outdoor glare is characterized by high luminance levels and differences of several orders of magnitude among different sources. Direct sunlight has an extremely

high peak luminance concentrated within a small angular extent, making it the most intense natural glare source in outdoor environments [7,17]. Although the luminance of building reflections is generally lower than that of the solar disc itself, specular glass, polished metal, and photovoltaic cover glass can concentrate solar radiation in specific directions, producing intense localized bright stimuli [9,13,21]. Using HDR images for field measurements of a specular-glass building, Suk et al. found that the luminance of façade-reflection hotspots ranged from 16,412 to 258,000 cd/m^2 [9]. Photographic luminance measurements of photovoltaic modules showed that luminance in non-glare regions was approximately 10^3 cd/m^2, whereas the center of a specular glare spot could exceed 10^8 cd/m^2 [21]. By contrast, rough surfaces such as ordinary concrete are dominated by diffuse reflection, which distributes reflected light over a larger solid angle and generally produces broad bright regions with relatively low peak luminance [22,23]. Relevant values and measurement conditions for different material surfaces are presented in Table 1, and typical reflection patterns are illustrated in Figure 1.

Table 1. Reflectance and luminance characteristics of outdoor reflective interfaces.

Material Interface	Reflectance Characteristics	Value	Value Type	Measurement or Calculation Conditions	Reference
Building façade with specular glass	Strongly directional specular reflection, producing localized high-luminance spots	16,412–258,000 cd/m^2	Reflected hotspot luminance	On-site measurement of an actual building in Los Angeles using HDR imaging	[9]
Performance glass with approximately 10% visible reflectance	Coexistence of specular and diffuse reflection	Approximately 1100 cd/m^2	Equivalent veiling luminance	Simulation under low solar elevation at the winter solstice, based on a road observation position	[24]
Low-reflectance glass with visible reflectance below 5%	Directional reflection is suppressed	Approximately 500 cd/m^2	Equivalent veiling luminance	The same solar position and road observation position as in the previous condition	[24]
Non-glare area of a photovoltaic module	Cover-surface reflection, with the viewing direction deviating from the specular direction	Approximately 10^3 cd/m^2	Module surface luminance	Image-based luminance measurement targeting the non-glare area of the module	[21]
Center of a photovoltaic-module glare spot	Highly concentrated specular reflection with pronounced luminance gradients	>10^8 cd/m^2	Local peak luminance	Image-based luminance measurement with the viewing direction close to the specular direction	[21]
Polished stainless-steel interface	Near-specular reflection, with reflected energy concentrated within a narrow range of outgoing angles	0.67–0.68	Integrated solar reflectance	Spectral reflectance measurement of stainless steel followed by integration over the solar spectrum	[25]
Metal-coated specular interface	Strong specular reflection, maintaining high reflectance even at large angles of incidence	0.85	Average solar reflectance	Spectral measurement of a metal-coated polyester mirror film for a scaled experiment involving a high-rise building façade	[26]
Ordinary newly constructed concrete	Rough surface dominated by diffuse reflection; reflected energy distributed over a large solid angle	0.35–0.40	Solar albedo	Solar-spectral reflectance measurement or on-site albedo measurement of concrete surfaces	[22,23]

Table 1. *Cont.*

Material Interface	Reflectance Characteristics	Value	Value Type	Measurement or Calculation Conditions	Reference
Aged concrete	Predominantly diffuse reflection; contamination, wear, and aging reduce overall reflectance	0.20–0.30	Solar albedo	Measurement of naturally exposed or aged concrete surfaces	[23]
Ordinary cement concrete with different mix designs	Predominantly diffuse reflection, affected by cement type, aggregate, and surface condition	0.18–0.35; average approximately 0.26	In situ albedo	On-site measurement of cement-concrete pavements using an upward- and downward-facing radiometric measurement system	[27]
High-reflectance precast concrete	Predominantly diffuse reflection with relatively high overall reflectance, but generally without concentrated specular highlights	0.27–0.60	Solar albedo	Spectral measurement over 300–2500 nm of precast-concrete specimens with different colors, mix designs, and surface treatments	[28]

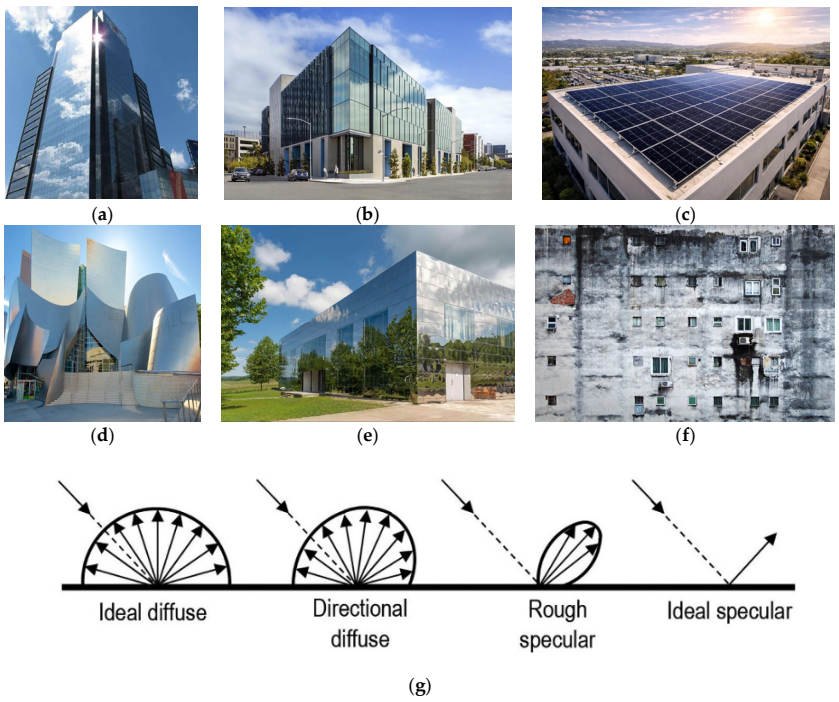


Figure 1. Typical solar-reflection patterns at different material interfaces: (**a**) specular-glass building façade; (**b**) low-reflectance glass; (**c**) building photovoltaic modules; (**d**) polished stainless-steel façade; (**e**) metal-coated specular interface; (**f**) concrete interface; and (**g**) typical directional reflection distributions of building-material surfaces.

Differences in the luminance produced by different materials essentially reflect differences in the directional distribution of reflected energy. A material's solar reflectance represents the overall proportion of incident radiation that is reflected but does not directly indicate luminance in a specific viewing direction. The integrated solar reflectance of polished stainless steel can reach 0.67–0.68 [25], overlapping with the albedo range of some highly reflective concrete surfaces, although the two materials produce distinctly different luminance distributions. Polished metal concentrates a greater proportion of reflected energy within a narrow specular direction and can therefore produce localized bright spots

at specific observer positions. Concrete disperses reflected energy across multiple directions and is less likely to generate directional peaks of comparable intensity [22,23,26–28].

Surface treatment and surface geometry also alter the directional distribution of reflected light. Polishing generally increases the specular component, matte and textured treatments can disperse reflected light, and concave surfaces may concentrate it within localized spaces [26]. However, these effects depend on the angle of incidence and viewing direction. Photovoltaic glass may still produce strong directional reflections at large angles of incidence [29,30], while reflective pavement coatings are not ideal diffuse reflectors and may contain both diffuse and specular components [31]. Glare risk therefore cannot be determined solely from overall reflectance or surface roughness. The actual luminance of a material surface should be evaluated in relation to its directional-reflection characteristics, the direction of solar incidence, surface geometry, and observer position.

Building surfaces that produce reflections also exhibit pronounced luminance non-uniformity. Solar reflections generally cover only localized portions of a façade, creating substantial luminance gradients among specular hotspots, transition zones, and non-reflective areas. Glazing units, assembled metal panels, reflective louvers, and photovoltaic arrays may also generate multiple discrete bright spots, causing luminance on the same surface to span several orders of magnitude [21,32,33]. Under these conditions, peak luminance can identify the strongest local stimulus but cannot represent the spatial extent of the bright region. Conversely, area-average luminance can characterize the overall level of the surface but may conceal the local peaks that actually cause glare. Comparative experiments using uniform and non-uniform light sources have further shown that different internal luminance distributions can produce different levels of discomfort glare even when their average luminance is identical [34]. Descriptions of outdoor-glare luminance should therefore jointly consider peak luminance, area-average luminance, the range of internal variation, and the angular area of bright regions to represent the actual luminance conditions and non-uniform characteristics of reflecting surfaces.

3.2. Spatial Geometry of Outdoor Glare

Daytime outdoor glare is not determined solely by the physical properties of high-luminance sources. Its formation and effects also depend on how light propagates through the built environment and on the relative positions of high-luminance sources and observers. When solar radiation reaches building and ground interfaces, its reflection is jointly influenced by interface orientation, surface inclination, building form, and surrounding obstructions, producing reflected light with different directions and spatial extents. Once these reflections reach the observer's location, their visual effects vary with viewing distance, gaze direction, position within the visual field, and the size of the high-luminance region. Accordingly, the spatial geometry of outdoor glare involves two continuous but distinct processes: first, the generation and propagation of high-luminance reflections through the environment; and second, the spatial manifestation of high-luminance regions after they enter the observer's field of view (Figure 2).

The surface geometry of building envelopes alters the normal direction at each point and thereby determines the propagation direction, coverage, and concentration locations of reflected light, making it an important component of glare formation geometry. Planar specular surfaces have relatively consistent surface normals, so reflected sunlight is generally directed toward a concentrated spatial direction. Convex surfaces have outward-varying normal distributions that disperse reflected light over a larger surrounding area, whereas concave surfaces may cause reflected rays from different locations to converge within a localized space, forming caustic lines or high-intensity reflection zones [8,26,35].

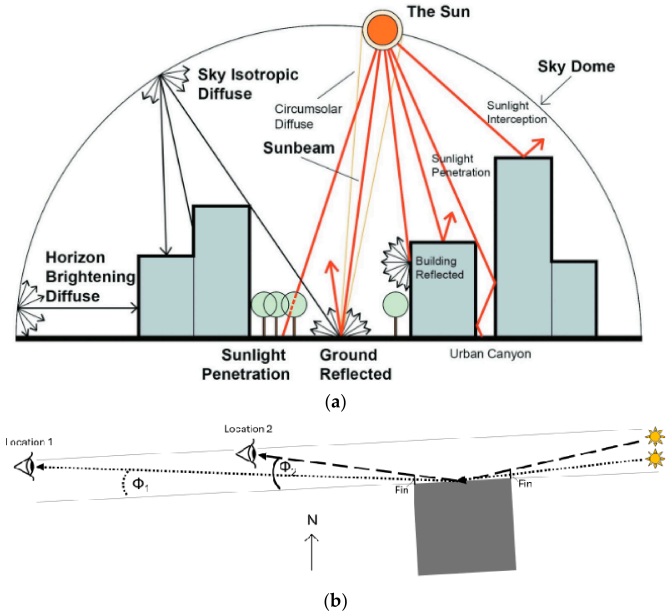


Figure 2. Spatial-geometric characteristics of the daytime luminous environment in the built environment. (a) Generation and propagation of high-luminance reflections [2], where the red lines indicate the incident and reflected paths of sunlight; (b) Spatial relationship when high-luminance areas enter the observer's field of view [24].

A comparison of planar, convex, and concave high-rise building models by Speroni et al. showed that, within a pedestrian-level measurement area of 6H × 1.5H, irradiance along reflected-light paths was 40–60% higher than in unaffected areas, while increases of 100–130% occurred at some edge-concentration locations [26]. Brzezicki's analysis of caustic lines similarly demonstrated that surface curvature alters both the locations at which reflected light reaches surrounding spaces and the degree of its concentration [35]. The resulting differences are manifested not only in reflection intensity but also in changes in the position, scale, and boundaries of glare-affected areas.

The effects of formation geometry also vary with the type and scale of human activity space reached by reflected light. In building-adjacent spaces, glare generally results from reflections cast by a single façade, entrance, or localized curved surface onto nearby ground areas and dwell locations, producing a relatively concentrated affected area. At the scale of streets and urban canyons, building height, street width, surface orientation, and obstructions on both sides jointly determine whether reflected light can reach sidewalks, carriageways, and buildings on the opposite side. Through ray-tracing analysis, Shih and Huang found that curtain-wall configuration, street width, period of solar exposure, and surrounding obstructions jointly alter the boundaries of areas affected by glass-curtain-wall reflections [8,36].

In open spaces such as plazas, reduced sky obstruction allows multiple building surfaces and ground pavements to produce bright reflections from different directions, expanding the affected area from a single light path to a combination of multiple reflection zones. When the direction of reflection aligns with a road or pedestrian route, the glare effect further expands from a localized space to continuous exposure along the route. At the street scale, Lee et al. analyzed 238 glass-curtain-wall buildings and 69 observation locations and found that the effects of solar altitude, building height, and façade tilt angle on reflected exposure varied with street orientation [3]. Reducing building height did not always mitigate exposure. Under some low-solar-altitude conditions, a lower building weakened the obstruction provided by buildings on the opposite side and could instead increase the likelihood that reflected light would reach observer locations. This finding

indicates that the effects of building scale must be evaluated in relation to street orientation and mutual obstruction rather than inferred solely from building height or façade tilt angle.

Glanville et al. simulated a 25 m-wide building façade and an adjacent road and found that reflected light at low solar altitudes could propagate along the road, exposing drivers to a potential risk of disability glare over part of their approach to the building [24]. At the larger urban-block scale, multiple buildings, different street orientations, and various reflecting surfaces may produce dispersed high-risk locations whose occurrence changes with the solar trajectory. Increasing spatial scale therefore not only expands the computational domain for reflected light but also transforms glare from a localized bright spot into spatial exposure associated with stationary activities, walking, cycling, and driving. Typical environments at different scales of human activity space are illustrated in Figure 3, while their principal formation conditions and glare-related differences are summarized in Table 2.

Table 2. Formation conditions and differences in outdoor glare across different spatial scales of human activity.

Spatial scale of Human Activity	Typical Spatial Extent	Dominant Formation Geometry	Typical Observers and Activities	Outdoor Glare Characteristics and Differences	Reference
Building-adjacent spaces	Approximately 1–20 m	A single façade or localized curved surface reflects light toward adjacent areas	Pedestrians at entrances and exits, people staying outdoors, and users of adjacent buildings	The impact range is concentrated; curved or inclined interfaces may produce localized focusing	[9,35]
Streets and urban canyons	Approximately 10–100 m	Façades on both sides reflect light toward the road and opposite buildings; reflection paths are constrained by street form and obstructions	Pedestrians, cyclists, and drivers	Reflection directions are influenced by street enclosure, making glare more likely to occur along specific street segments and during specific periods	[8,37]
Public open spaces	Tens to hundreds of meters	Surrounding façades, paving, and facilities produce multidirectional reflections	People staying in the space, pedestrians, and participants in public activities	The number and visible range of high-luminance sources are relatively large; their effects vary with position and orientation	[26]
Roads and continuous activity paths	Hundreds to thousands of meters	Reflected-light paths overlap with movement paths	Drivers, cyclists, and pedestrians	Glare appears, intensifies, persists, and disappears as observers move through space	[24,38]
Urban blocks and districts	Hundreds to thousands of meters	Multiple buildings and different street orientations form a network of reflection paths	People across different street segments and public spaces	Risk is distributed discontinuously across space and time, concentrating around specific buildings, street segments, and periods	[38,39]

Once reflected light reaches the area occupied by an observer, its effect depends on the position and scale of the bright source within the field of view. In this review, this level of spatial relationship is defined as observer geometry. Figure 2b illustrates the relationships among the sun, the reflecting surface, and different observer positions. Observer movement changes the angle between the reflected light and the line of sight, causing the same bright surface to be invisible, visible in the peripheral field, or located near the visual axis at different positions. Whereas formation geometry concerns whether light can reach a particular space, observer geometry concerns how a bright stimulus that has reached that

space enters the observer's field of view. It is primarily described by viewing distance, viewing direction, glare-source eccentricity angle, solid angle, and visual-field orientation. Existing glare models have been developed mainly for the latter type of spatial relationship. Figure 4 illustrates the solid angle subtended by the glare source and its angular position within the visual field; definitions of the relevant geometric quantities and representative evaluation equations are provided in Appendix A.1. Hopkinson found that discomfort glare varied with the angle between the glare-source direction and the line of sight [40]. On this basis, Luckiesh and Guth proposed the position index to represent the relative position of a light source within the visual field [41]. Hopkinson and Petherbridge subsequently incorporated the position index into a glare-index model to predict discomfort using source luminance, background luminance, solid angle, and position within the visual field [42]. Subsequent discomfort-glare models have largely retained this general formulation [43–46].



Figure 3. Typical built environments at different spatial scales of human activity: (**a**) building-adjacent spaces; (**b**) streets and urban canyons; (**c**) public open spaces; (**d**) roads and continuous activity paths; and (**e**) urban blocks and districts.

Unlike observer geometry, which has been incorporated into existing glare models through eccentricity angle, solid angle, and position index, formation geometry has not yet been represented by a unified quantitative framework. Existing studies have incorporated building height, façade tilt angle, street orientation, and obstruction relationships into reflected-exposure analyses and have begun to compare the combined effects of these factors [3,39]. However, their effects and correspondence with risk categories remain dependent on the specific model, viewing direction, and scenario configuration. It is therefore difficult to establish a quantitative representation that supports direct comparisons across spatial scales and maintains a stable relationship with observer responses.

The effects of individual factors also vary with spatial scale. Local curvature and tilt angle influence the concentration of reflected light near buildings; street morphology and obstructions determine the propagation range of light; path orientation affects the distance over which glare persists; and urban-block layouts control the spatiotemporal distribution of risk. Results obtained for a single building or observation point cannot be directly extrapolated to other spatial scales. The assessment of formation geometry must therefore be conducted in relation to the specific space and its dominant factors.

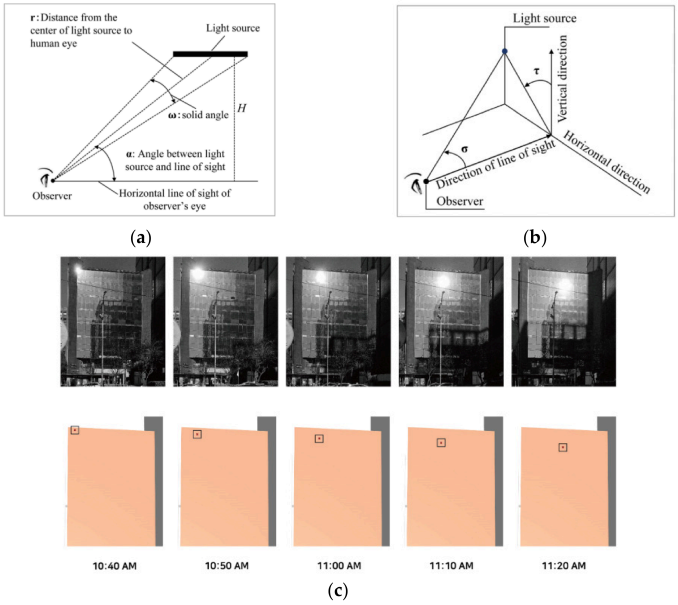


Figure 4. Observer geometry. (**a**) Solid angle of the glare source, ω; distance from the eye to the center of the source, r; and angle between the source direction and the horizontal line of sight, α. (**b**) Horizontal position angle of the source, σ, and angle between its direction and the vertical direction, τ. (**c**) Changes in observer geometry for reflected glare caused by solar movement.

3.3. Forms of Outdoor Glare

Daytime outdoor glare does not exhibit a uniform form within the field of view. By synthesizing the approaches used in previous studies to identify the sun, building reflections, photovoltaic surfaces, and non-uniform light sources, this review classifies bright regions into three basic forms according to their boundaries, scale, number, and degree of continuity: concentrated highlights, continuous-area highlights, and discrete-patch highlights [9,13,32,35,47,48]. This classification is not an established typology in existing glare standards but a synthesis of different outdoor high-luminance structures. In actual built environments, the three forms may coexist, producing a composite luminance field composed of local peaks, large-area bright surfaces, and multiple discrete reflection patches [9,13,32]. Compared with luminaire sources that have clearly defined boundaries and relatively stable dimensions, outdoor bright regions are jointly influenced by solar direction, surface geometry, material reflection, and observer position. Their form and position within the field of view therefore vary across time and space, as illustrated in Figure 5 [35,48].

Direct sunlight is a typical form of concentrated highlight, characterized by a small angular extent and extremely high peak luminance. When it enters the field of view, it produces a pronounced local luminance discontinuity [7,17]. Specular reflections from glass, polished metal, and building-integrated photovoltaic surfaces may also form small bright spots, although their position, size, and duration are constrained by the direction of solar incidence and observer geometry [9,13,21]. This form of glare is characterized primarily by reflected energy concentrated within a small angular extent rather than by a large affected area. Geisler-Moroder and Knoflach noted that DGP is particularly sensitive to small but extremely bright sources, such as the sun and specular reflections. Its calculation is also affected by the scale used for source identification and by image resolution, requiring a minimum solid-angle correction that varies with the source position in the field of view [48]. Using only the surface-average luminance to describe concentrated highlights may conceal local peaks, whereas an excessively large source-identification threshold may omit small but extremely bright reflected spots.

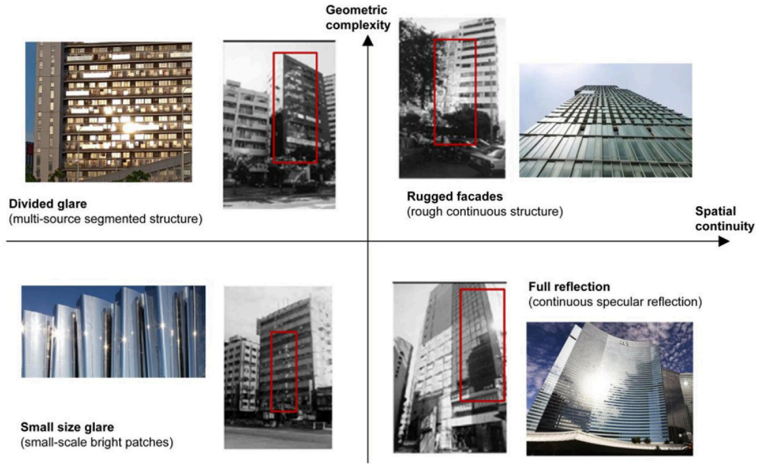


Figure 5. Common forms of daytime outdoor glare in the built environment. The red boxes highlight specific areas on the building facade that correspond to the glare forms shown in the figure.

Continuous-area highlights are produced primarily by large glass curtain walls, light-colored façades, highly reflective pavements, or bright skies. Although their peak luminance may be lower than that of direct sunlight, these bright regions can occupy a large angular extent and expose observers to a persistently high-luminance background [49,50]. A continuous bright area is not necessarily uniform in luminance; actual building surfaces often contain luminance gradients, local peaks, and distinct boundaries between bright and dark regions. Relevant studies have shown that the local background, internal luminance distribution, and shape of a large-area source can alter glare perception. Its visual effects therefore cannot be fully described using only the total solid angle and average luminance [32,34,49]. Representing an entire surface as a single uniform source preserves its total area and average luminance but eliminates internal luminance differences, making it difficult to distinguish a uniformly bright surface from an intense local reflection embedded within a darker surface.

Façade subdivisions, shading devices, partial obstructions, and multiple reflective surfaces can cause outdoor glare to appear as discrete patches or array-like structures. Studies of multiple and non-uniform light sources indicate that several bright regions may be adjacent and perceived as a single entity or dispersed across different positions in the field of view, forming multiple potential glare centers [32,34,46,47]. Experiments with non-uniform sources have further shown that a point-array source composed of multiple bright elements may cause greater discomfort than a uniform source with the same average luminance, indicating that the spatial arrangement of bright elements cannot be fully represented by total area alone [32,34]. The effects of multi-source glare may also depend on the number of patches, their angular spacing, arrangement direction, and degree of clustering. Combining adjacent patches into a single source may enlarge the equivalent area and reduce the average luminance, whereas calculating them entirely separately may overlook their perceptual integration.

4. Effects of Outdoor Glare

The effects of outdoor glare on observers are manifested primarily as visual discomfort and impaired visual function. The CIE defines glare as a visual condition in which an unsuitable distribution or range of luminance, or extreme contrast, causes discomfort, reduces the ability to recognize important objects, or produces both effects [51]. Accordingly, glare is generally classified as discomfort glare or disability glare. The former describes the discomfort and acceptability associated with bright stimuli, whereas the latter occurs when veiling luminance produced by intraocular scattering reduces target contrast and

recognition performance [52,53]. In this review, the impact process is summarized in three interrelated stages: physical stimulus, glare sensation, and perception and judgment. As illustrated in Figure 6, scene luminance, contrast, and spatial geometry constitute the external stimuli; the visual system produces corresponding responses; and the observer forms a judgment based on adaptation state, visual task, and environmental context.

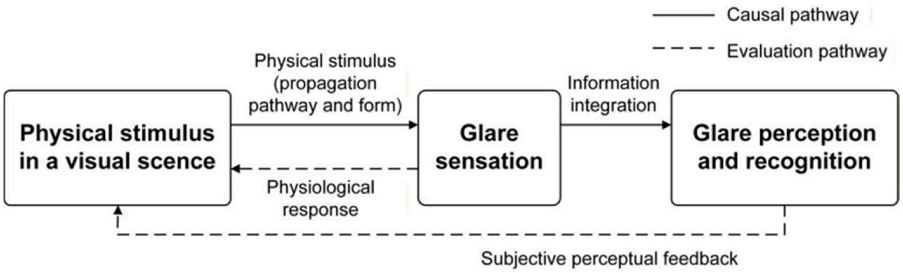


Figure 6. Glare perception pathway.

4.1. Visual Function and Task Performance

The effect of daytime outdoor glare on visual function is manifested primarily as a reduction in the effective contrast of visual targets. Bright stimuli produced by direct sunlight and reflections from buildings, ground surfaces, and windshields generate equivalent veiling luminance through intraocular scattering, making target outlines and details more difficult to distinguish. The magnitude of this effect depends on target characteristics. High-contrast targets can generally still be recognized, although additional time may be required, whereas low-contrast or small targets and those located against complex backgrounds are more likely to be missed. Age-related increases in intraocular scattering and reductions in visual sensitivity can further amplify these effects [54,55].

Impaired visual function can subsequently affect continuous movement tasks. When the low-angle sun is close to the direction of travel, pedestrians, vehicles, traffic signs, and road obstacles may temporarily lose visibility within a limited viewing distance, causing recognition delays that result in insufficient time for steering, avoidance, or braking. Glare-induced task interference is also strongly directional and stage-dependent, with its effects often concentrated along specific road orientations, at intersections and turning points, and during limited periods around sunrise and sunset. Observers may compensate by reducing speed or redirecting their gaze, but the degree of compensation varies among individuals and cannot fully eliminate the safety risks associated with the loss of visual information [10,55]. Eye-tracking and traffic-sign recognition experiments conducted on actual roads have further linked solar-glare exposure to the attenuation of available sight distance, providing quantitative evidence of visual effects under specific driving tasks [56]. Table 3 summarizes representative evidence concerning the effects of daytime outdoor glare on target detection, driving operations, and crash outcomes.

Existing studies have demonstrated the effects of outdoor glare at three levels: visual recognition, operational responses, and crash outcomes. However, the relationships among these levels have not been adequately validated across different spaces, light-source types, and observer tasks. Longer reaction times do not necessarily result in crashes, changes in speed may include active driver compensation, and crash severity cannot be used to directly infer losses in visual function. Existing evidence has primarily focused on drivers and low-angle sunlight, while windshield reflections, simulation experiments, and traffic-crash data represent substantially different exposure conditions. By contrast, direct measurements remain limited regarding the effects of glare from building façades, photovoltaic surfaces, and highly reflective ground surfaces on the visual tasks of pedestrians, cyclists, and people remaining in outdoor spaces. Although the visual effects of daytime outdoor glare have

been broadly established, their effect thresholds, duration, and variations across different spatial and population conditions remain unclear.

Table 3. Effects of daytime outdoor glare on visual function and task performance.

Daytime Outdoor Context and Glare Condition	Evaluation Measures	Main Findings	Reference
Daylight-induced reflection of the dashboard on the windshield, producing veiling luminance	Pedestrian-detection reaction time; miss rate	High-contrast targets mainly showed delayed responses, whereas missed detections increased for low-contrast targets	[54]
Intersection turning under simulated low-angle sunlight	Safe turning time; number of collisions	Solar glare shortened the safety margins retained by drivers and increased collisions; the effects were more pronounced among older drivers	[55]
Low-angle solar glare under different road orientations	Vehicle speed; speed variability	Speed variability increased under glare conditions, with the extent of the increase moderated by road orientation and traffic demand	[10]
Daytime pedestrian crashes in Taiwan, 2003–2016	Pedestrian-crash fatality outcomes	Solar glare was associated with the risk of pedestrian fatalities, which was also influenced by road, vehicle, age, and driving-behavior factors	[14]
Direct-sun glare on a two-lane highway	Driver gaze distribution, traffic-sign recognition distance, and attenuation of available sight distance	An estimation method for available sight distance under glare conditions was developed based on eye-tracking and traffic-sign recognition experiments; the results are applicable to the road and task conditions examined in the study	[56]

4.2. Perceived Discomfort and Environmental Evaluation

Compared with impaired visual function, perceived discomfort depends not only on the intensity of bright stimuli but also on the directionality of reflection, the boundaries of bright regions, the observer's position, and individual judgment. Concentrated and sharp specular reflections are more likely to cause glare and avoidance, whereas large-area bright surfaces may reduce overall visual comfort by occupying a substantial proportion of the field of view, further affecting spatial legibility and environmental acceptability [9,57–60]. Outdoor glare perception is primarily measured using glare categories, comfort ratings, and multidimensional questionnaires. Glare categories determine whether a stimulus reaches perceptible, disturbing, or intolerable levels; comfort scales reflect the overall visual experience; and multidimensional questionnaires extend the assessment to sensitivity, disorientation, and avoidance tendencies. Table 4 summarizes the scale formats and main findings reported in relevant studies.

The rating scales used in existing studies are not standardized, and different instruments vary in their evaluation targets, number of response categories, and semantic anchors. Glare-category scales emphasize the immediate disturbance caused by bright stimuli, comfort scales encompass broader environmental experiences, and multidimensional questionnaires may additionally incorporate thermal sensation, architectural preferences, and psychological responses. Directly comparing these results may introduce semantic inconsistencies in the interpretation of glare and systematic shifts in assessment outcomes, thereby reducing comparability across studies.

The available evidence also has spatial and behavioral limitations. Field surveys are generally concentrated at a small number of observation locations, image-based questionnaires do not reproduce actual luminance conditions or dynamic exposure, and some studies have applied different statistical methods to the same or related datasets, leaving a

limited body of independent evidence. Existing findings indicate that building reflections affect perceived discomfort and environmental appraisal, but they do not yet adequately explain how discomfort emerges, intensifies, and subsides across continuous space.

Table 4. Methods for assessing perception and environmental evaluation of reflected daytime outdoor glare.

Scenario	Assessment Dimensions	Scale or Instrument	Main Findings	Reference
Pedestrians around reflective buildings	Glare and visual comfort	Four-category glare scale; seven-point comfort scale ranging from −3 to +3	Perceptible glare was reported by 36.6% of respondents, while 13.4% reported disturbing glare	[9]
Different reflective materials	Reflection characteristics and visual discomfort	Glare categories and comfort ratings	Reflectance and specularity jointly affected discomfort	[60]
Areas surrounding reflective buildings in Kuala Lumpur	Sensitivity and avoidance	Structured multi-item questionnaire	Façade reflections were associated with pedestrian visual comfort and avoidance	[57]
A related dataset comprising 500 survey responses	Sensitivity, exposure, and avoidance	Multi-item questionnaire and latent-variable analysis	Different statistical models consistently supported the relationships among the variables	[58]
Images of metallic and glass reflective façades	Discomfort, disorientation, and environmental perception	Image stimuli and a Likert-scale questionnaire	Sharp metallic reflections caused greater discomfort and disorientation	[59]

4.3. Behavioral Responses and Spatial Use

Behavioral responses to outdoor glare are jointly influenced by patterns of spatial use and activity constraints. In spaces intended for stationary activities, such as plazas, rest areas, and building entrances, observers may reduce the stimulus by turning their heads, shielding the bright source, changing their orientation, or relocating, and may further adjust their seating or dwell location. On pedestrian streets and in commercial pedestrian areas, the spatial relationship between the observer and the bright source changes continuously. Looking downward, averting the gaze, or choosing the shaded side may reduce glare exposure, but these responses may also limit the observation of pavement conditions, traffic signals, and other pedestrians. On motor-vehicle roads and at intersections, predetermined routes and driving tasks constrain positional adjustments; drivers may therefore compensate primarily by reducing speed, redirecting their gaze, or modifying driving operations. These behavioral responses are highly context-dependent, but the strength of the available evidence is uneven. Existing studies have primarily examined this process through avoidance tendencies, changes in driving operations, and crash outcomes. Representative evidence is summarized in Table 5.

Existing evidence indicates that outdoor glare can induce avoidance tendencies and compensatory driving behavior, but support for actual changes in spatial use remains limited. Evidence of pedestrian avoidance is derived primarily from self-reported tendencies in questionnaires [57,58] and has not yet been validated through observations of dwell time, seat relocation, or walking trajectories. Although façade continuity, spatial openness, and shading conditions may vary concurrently with location and route choices, few studies have simultaneously measured glare, thermal conditions, and actual behavior. Consequently, observed differences in spatial use cannot be directly attributed to bright-light stimuli.

Table 5. Behavioral responses to daytime outdoor glare and its effects on spatial use.

Spatial Context and Study Subjects	Behavioral Indicators	Main Findings	Reference
Pedestrians around reflective buildings	Survey-reported avoidance tendency	Avoidance mediated the relationship between glare occurrence periods and sensitivity	[58]
Vehicles driving toward a low-angle sunset	Vehicle speed and speed fluctuations	Drivers reduced speed only slightly, while speed variability increased	[61]
Actual roads with different orientations	Degree of speed dispersion	Speed variability was higher during solar-glare periods than during non-glare periods	[10]
Urban signalized intersections	Crash occurrence and type	Crashes at intersections were more concentrated when the solar direction was close to the road direction	[62]
Daytime pedestrian traffic crashes	Proportion of pedestrian-crash fatalities	The proportion of fatalities in glare-related crashes was 2.46%, higher than the 1.83% observed in non-glare crashes	[14]
Roadside photovoltaic visual settings	Vehicle speed, acceleration, and steering operations	Driving operations changed under different sunlight and road-geometry conditions, but the effects of glare were not isolated	[63]

Traffic studies provide relatively objective data on driving operations and crash outcomes, but these indicators are located downstream in the behavioral-response chain. Driving-simulation research on roadside photovoltaic settings has found changes in driving operations under different sunlight and road-geometry conditions [63]. However, the study did not isolate the effects of glare, and the observed changes may also have been influenced by the visual salience of the installations, road geometry, and active driver compensation. Changes in speed and vehicle control therefore cannot be directly equated with glare-induced losses of visual function. Crash occurrence and severity are also affected by traffic flow, road configuration, vehicle characteristics, and individual factors. Overall, research on the relationship between daytime outdoor glare and spatial use still lacks continuous observations linking actual exposure and immediate avoidance to subsequent changes in dwell time and travel routes.

5. Evaluation Methods for Daytime Outdoor Glare

5.1. Geometric-Path-Based Glare-Risk Assessment

Daytime outdoor glare is subject to clearly defined conditions of spatial reachability. Actual exposure occurs only when direct sunlight or surface-reflected light enters the observer's field of view along a specific path. When complete luminance data are unavailable during the planning stage, or when large urban areas must be screened, the potential locations, directions, and periods of glare can be determined from solar position, road and building orientation, surface geometry, spatial obstructions, and the observer's line of sight. Direct-glare assessment primarily examines the relationships among solar trajectories, spatial obstructions, and viewing direction. Relevant methods have evolved from angular assessments of individual road segments to spatiotemporal mapping of road networks using GIS, digital surface models, and street-view imagery [15,38,64]. Reflected-glare assessment must additionally resolve two light paths—from the sun to the reflecting surface and from the reflecting surface to the observer—and identify affected spaces using reflected-area boundaries, forward or backward ray tracing, and annual hit mapping [8,39,65–67]. Some studies have further incorporated HDR luminance measurements and material directional-reflection data, extending the assessment from geometric reachability to an integrated evaluation of light paths and stimulus intensity [13,26,68]. Representative methods are summarized in Table 6.

Table 6. Geometric-path-based evaluation of daytime outdoor glare risk.

Type	Scenario	Method	Core Criteria and Outputs	Reference
Direct glare	Intersections, ramps, and tunnel exits	Road-alignment and solar-trajectory calculations	Angle between the sun and the line of sight; identifies risk dates and periods	[64]
	Urban road network	GIS and spatial-obstruction analysis	Road orientation, slope, and solar position; identifies at-risk road segments	[15]
	Urban roads	Street-view imagery overlaid with solar trajectories	Viewing angle and street obstructions; identifies risk locations and periods	[38]
	Road driving under natural daylight	Visual experiments and geometric calculations	Horizontal and vertical recognition angles; determines acceptable angular boundaries	[12]
	Urban and interurban roads	Mobile and airborne laser-scanning point clouds and solar-geometry calculations	Integration of driving direction, road gradient, and environmental obstructions; identification of risk locations and periods	[69]
	Bus stops	Mobile laser-scanning point clouds, solar-path analysis, and vegetation-obstruction scenario analysis	Calculation of solar paths and obstruction periods; comparison of the mitigation effects of different tree sizes and locations	[70]
Reflected glare	Areas surrounding glass curtain walls	Field measurements and geometric simulation	Reflection-region boundaries; identifies affected spaces	[8,65]
	Ultra-high-rise glass curtain walls	Year-round ray tracing	Reflected-light paths and ray-hit locations; produces the annual risk distribution	[66]
	Areas surrounding curtain-wall buildings	Forward and backward ray tracing	Reflection sources and observer viewsheds; identifies affected areas	[67]
	High-rise business districts	Street-view imagery, solar trajectories, and obstruction analysis	Reachability of reflected-light paths; produces the spatiotemporal distribution	[39]
	Urban streets with a high concentration of glass curtain walls	Backward ray tracing and parametric scenario analysis	Street orientation, building height, façade tilt angle, and viewing conditions; identification of potential exposure locations and reflection sources	[3]
Integrated	Airport photovoltaic arrays	Ray tracing and HDR measurements	Reflected-light paths and a threshold of 30,000 cd/m^2; identifies risk periods and locations	[13]
	Pedestrian level around high-rise buildings	Scaled physical-model experiments	Reflected-light paths and local concentration; identifies areas of irradiance concentration	[26]
	Road-adjacent photovoltaic installations	Directional-reflection measurements and annual solar-reflection calculations	Reflection direction, surface luminance, and viewing direction; identification of risk periods	[29]
	Two-lane highway	Ray-obstruction analysis, an eye-tracking-based field-of-view model, and traffic-sign recognition experiments	Relationships among solar position, illuminance, obstruction, and sight-distance attenuation; estimation of available sight distance under glare conditions	[56]

Direct glare in road environments is characterized by a clearly defined solar position and a viewing direction constrained by road alignment, making it suitable for geometric assessment based on solar trajectories, road orientation, and obstruction relationships. Calculations for individual road segments can identify risk periods at intersections, ramps, and tunnel exits with reasonable accuracy. GIS- and street-view-based methods can extend the assessment to road networks, while mobile and airborne laser-scanning point clouds can further represent driving trajectories, road gradients, and environmental obstructions to identify the locations and periods in which direct sunlight enters the field of view [69]. However, these methods generally continue to rely on predefined lines of sight and uniform angular thresholds, making it difficult to fully account for turning maneuvers, head

movements, and individual visual differences. The scalability of geometric methods is therefore achieved by simplifying observer behavior, and their outputs are more suitable for representing the extent of potential exposure than the actual severity of glare.

Building-reflection scenarios involve two light paths: one from the sun to the reflecting surface and another from the surface to the observer. They therefore require more detailed descriptions of surface orientation, curvature, and material properties. Reflected-area boundaries are suitable for rapidly delineating the affected area of a single curtain wall; forward ray tracing facilitates analysis of the spatial propagation of reflected light; and backward ray tracing is more appropriate for identifying potential reflection sources from observer positions on roads or in public spaces. Annual ray tracing can additionally estimate the frequency and duration of glare events, although its results depend strongly on building-model accuracy, surface normals, and the directional-reflection parameters of materials. Incorporating HDR luminance data or intensity thresholds can bring the assessment closer to actual visual risk but may reduce its general applicability, because luminance thresholds developed for specific airport tasks may not be applicable to pedestrians, drivers, or general public spaces. Recent studies have further integrated directional-reflection measurements or visual-task data into geometric analyses, extending assessment from path identification to reflected-luminance estimation and the prediction of available sight distance under glare conditions [29,56]. Nevertheless, identifying potential exposure is not equivalent to determining its actual effects. Assessment must also consider exposure duration, time of occurrence, the sensitivity of affected observers, and cumulative effects from multiple sources [71]. No single method is optimal for every setting: large-scale screening may prioritize geometric reachability, whereas detailed assessments of critical areas should additionally incorporate photometric conditions, visual tasks, and dynamic exposure.

5.2. Scenario-Based Evaluation Using Mathematical Models

Research on daytime outdoor glare still lacks universally applicable evaluation metrics specifically calibrated for such conditions. Current applications largely rely on models developed for indoor daylighting, electric lighting, and road lighting. Because these metrics were originally established under different luminance ranges, source configurations, visual tasks, and subjective rating scales, their numerical values and category thresholds cannot be directly adopted as absolute criteria for daytime outdoor environments. Daylight Glare Probability (DGP), Daylight Glare Index (DGI), and Unified Glare Rating (UGR), which are currently among the most widely used metrics, account for source luminance, solid angle, position within the field of view, and background conditions once the observer position and viewing direction have been specified. They can therefore be used for relative comparisons among different locations, periods, and design alternatives within the same scene [60,72–74]. More recently, the applicability of UGR and its modified form UGR′, which accounts for non-uniform source luminance, has been examined for outdoor residential luminaires. The results showed that the calculated values are affected by factors including the delineation of the luminous area, the blurring parameter, viewing angle, and background luminance, while the corresponding rating scales still require further validation through psychophysical experiments [75]. Representative metrics and their original conditions of applicability are summarized in Table A1 in Appendix A.2.

In practice, luminance distributions within the field of view are usually obtained using high-dynamic-range (HDR) photography or lighting simulation. The sun, reflecting façades, and high-luminance areas on the ground are then identified, and their luminance, solid angle, position, and background conditions are entered into existing models [60,76,77]. Similar simulation procedures have also been applied to architectural daylighting design, where combinations of shading devices, light shelves, and skylights are compared to assess

daylight utilization while controlling glare [78]. Recent studies have further incorporated temporal variations in measured luminance, the relative positions of reflecting sources and moving observers, and parametric building geometry into continuous calculations, using existing glare indices or data-driven models to compare different periods and design scenarios [79–81]. These methods can convert potential exposure locations identified through geometric path analysis into continuous indices. However, they primarily demonstrate the computational applicability of these models and their ability to support relative comparisons in outdoor settings; they do not establish that the original discomfort categories retain the same perceptual meaning outdoors.

In outdoor electric-lighting and quasi-outdoor experiments, discomfort-glare modeling has expanded from a single rating to the representation of individual differences and dynamic stimuli. Probabilistic models can estimate the likelihood of different discomfort ratings [82], while cross-dataset comparisons indicate that direct illuminance at the eye from a glare source can, under certain conditions, serve as a readily obtainable simplified predictor [83]. For nighttime pedestrian lighting, studies have also recommended the standardized reporting of photometric stimuli and viewing conditions to facilitate comparisons among different discomfort-glare models [84]. Experiments involving cyclic light sources have shown that repeated variations in a stimulus do not necessarily increase discomfort, with significant differences occurring only under certain low-frequency luminance variations [85]. Models based on the human visual system have further incorporated processes such as visual adaptation [86]. These studies provide useful directions for evaluating daytime outdoor glare, although their findings still require validation under conditions involving direct sunlight and reflections from buildings.

The principal limitation in transferring these models arises from the differences between their original calibration conditions and the luminance structures encountered outdoors. A daytime outdoor field of view may simultaneously contain the sun, sky, buildings, and ground reflections, while observer movement continuously alters the boundaries and positions of high-luminance areas within the field of view as well as the observer's adaptation state. Different methods of glare-source segmentation can also change the source solid angle, background luminance, and resulting index value. Existing studies have improved the contextual adaptability of these models by modifying glare-source identification methods and minimum solid-angle criteria or by incorporating variables such as solar angle, reflector dimensions, building geometry, observer movement, and material roughness [3,33,48,74,80,81,87]. However, such adjustments cannot replace the validation of perceptual validity. The same index value may not correspond to the same degree of discomfort in indoor window, direct-sunlight, and building-reflection conditions. Future studies should therefore determine the limits of model applicability by examining subjective perception, visual performance, and behavioral responses across different spatial settings, visual tasks, and population groups.

6. Discussion and Conclusions

Existing studies indicate that some glare metrics can distinguish differences in glare among locations, periods, or design alternatives when the observer position, viewing direction, and luminous environment remain relatively stable [60,72–74,87]. Source luminance, solid angle, background luminance, and position weighting in existing models can still describe the principal stimulus characteristics at a given moment. However, the applicability demonstrated in current outdoor studies primarily concerns relative comparisons at static viewpoints or discrete moments and does not imply that the original category thresholds can be directly applied to daytime outdoor environments. Although recent studies have incorporated temporal variations in measured luminance, the relative positions of

reflecting sources and moving observers, and parametric building geometry into dynamic calculations [79–81], thereby extending the representation of the glare-exposure process, the corresponding perceptual categories and behavioral validity have yet to be directly verified. Solar movement, obstruction by buildings, and surface reflections continuously alter the intensity, direction, and extent of high-luminance areas, while observer movement changes the viewing direction, target distance, and task requirements. Consequently, the same instantaneous index value may have different effects depending on exposure duration, direction of approach, and task stage.

The limitation of a single metric is not that it cannot describe outdoor glare, but that it cannot readily encompass spatial accessibility, stimulus intensity, the exposure process, and observer responses simultaneously. Geometric metrics are suitable for identifying potential exposure locations and periods; photometric quantities and glare indices are appropriate for quantifying instantaneous stimuli; and subjective assessments, visual-task measures, and behavioral indicators reflect actual effects at different levels. Compressing these results into a single universal value may obscure differences among glare forms, activity patterns, and population responses. Daytime outdoor glare is therefore better evaluated using a hierarchical and type-specific framework. While retaining the role of existing metrics in static evaluation, the relevant parameters should be selected according to whether the glare is direct or reflected, whether the observer is stationary or moving, and the type of visual task involved. Evaluation results should then be updated in accordance with changes in the physical environment and the observer's movement path.

Based on the above analysis, future research on daytime outdoor glare evaluation may proceed along two interrelated pathways: dynamic light-stimulus research and response-and-evaluation research, as illustrated in Figure 7. The former focuses on the spatial distribution of multiple high-luminance sources and the dynamic exposure process, whereas the latter examines the relationships between physical stimuli and observer responses and the context-specific improvement of evaluation methods. These two lines of research should be integrated under consistent definitions of glare sources, spatial scales, and observer tasks, and should jointly support glare-risk determination, design-scheme evaluation, and the design of buildings and outdoor environments.

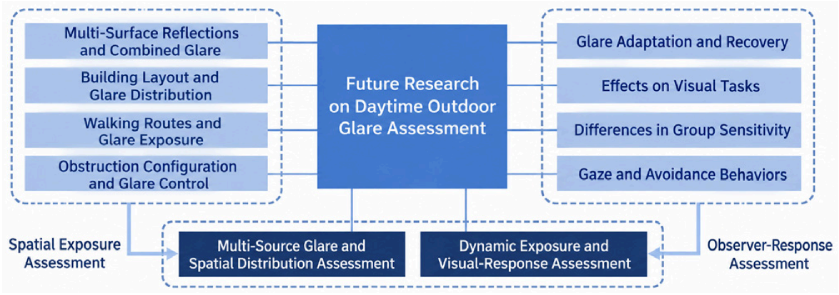


Figure 7. Future research directions and application pathways for daytime outdoor glare assessment.

In design applications, solar position, spatial obstructions, and viewing directions can be considered together to identify critical surfaces that direct sunlight or reflected high-luminance stimuli toward major pedestrian routes, vehicular routes, and occupied areas. Materials, façade geometries, and shading strategies can then be compared accordingly. Material selection should consider directional reflection within the actual range of solar incidence angles; glare risk cannot be determined solely from overall reflectance, anti-reflective coatings, or frosted finishes [29–31]. Façade orientation, tilt angle, and curvature should be evaluated in relation to annual solar paths and sensitive observer locations, while geometric modifications should also be examined to determine whether they redirect reflections toward other occupied spaces [3,81]. In existing spaces, localized shading devices,

screens, or vegetation may be introduced along critical exposure paths. However, their actual effectiveness in reducing stimulus intensity, affected area, and exposure duration should be verified through scenario-based simulations or field measurements [70].

In addition to outdoor reflections, glazing systems should also account for the effects of transmitted light on indoor daylighting and glare. The scattering properties of aerogel glazing can alter indoor daylight distribution and glare evaluation, while the spectral differences among tinted glazing systems may cause actual discomfort to deviate from the predictions of existing metrics [88–90]. External shading strategies for residential buildings must likewise balance usable indoor daylight with discomfort-glare control [91]. Because these studies address indoor luminous environments, their findings cannot be directly used to assess outdoor glare reflected from façades. The effects of glazing systems on the indoor and outdoor environments must therefore be evaluated separately.

This paper synthesizes research on daytime outdoor glare from three perspectives: physical characteristics, observer effects, and evaluation methods. The main conclusions are as follows:

1. Daytime outdoor glare is characterized by high luminance, multiple sources, non-uniformity, and temporal variability. Solar movement, building obstructions, interface form, and material reflectance jointly alter the intensity, direction, scale, and number of high-luminance regions. Fixed viewpoints and single luminance values cannot represent complete exposure conditions.
2. Outdoor glare can cause visual discomfort and impaired visual function and may induce immediate behavioral adjustments. Existing evidence has primarily focused on subjective evaluations, target recognition, and compensatory driving behavior, whereas direct observations of dwell time, detouring, location choice, and spatial patterns of use remain limited.
3. Existing assessment approaches have gradually evolved from geometric-path identification and the application of established glare indices toward integrated analyses of directional reflection, dynamic exposure, and visual tasks. Different studies have incorporated moving observers, directional reflection, and parametric building geometry into their assessments, and some have established links between physical exposure and available sight distance in specific driving tasks. However, the applicability of these relationships across different light-source types, spatial scales, and observer groups remains to be validated.
4. The evaluation of daytime outdoor glare needs to connect dynamic physical exposure with observer responses. Future research should simultaneously record the luminance, direction, scale, visual-field position, and duration of multisource high-luminance stimuli, and examine perceptual, visual-performance, and behavioral outcomes across different spaces, tasks, and population groups. This will support the development of hierarchical and differentiated evaluation methods suitable for dynamic outdoor environments.

Author Contributions: Conceptualization, Y.H. and J.X.; methodology, Y.H., H.Y. and J.X.; investigation (literature search and screening), Y.H., H.Y., Y.C., A.Y. and Y.W.; formal analysis, Y.H. and H.Y.; data curation (evidence extraction and organization), H.Y., Y.C., A.Y. and Y.W.; visualization, Y.H. and H.Y.; writing—original draft preparation, Y.H.; writing—review and editing, Y.H., H.Y., Y.C., A.Y., Y.W. and J.X.; supervision, J.X.; project administration, J.X.; funding acquisition, J.X. All authors have read and agreed to the published version of the manuscript.

Funding: This research was funded by the National Natural Science Foundation of China, grant number 52478077.

Data Availability Statement: No new data were created or analyzed in this study. All information synthesized in this review was derived from publicly available publications and databases, and all sources are cited in the manuscript.

Conflicts of Interest: The authors declare no conflicts of interest. The funders had no role in the design of the study; in the collection, analyses, or interpretation of data; in the writing of the manuscript; or in the decision to publish the results.

Appendix A

Appendix A.1. Geometric Quantities in Figure 4 and Representative Evaluation Equations

For a high-luminance region subtending a small angular extent within the field of view, its solid angle can be approximated as:

$$\omega \approx \frac{A_{\text{proj}}}{r^2} \tag{A1}$$

where ω is the solid angle subtended by the glare source at the observer's eye, A_{proj} is the projected area of the high-luminance region facing the observer, and r is the distance from the observer's eye to the source. Equation (A1) is a small-angle approximation. For large-area curtain walls or reflecting regions with complex geometries, the solid angle should be determined from the actual visible area.

Taking the Unified Glare Rating (UGR) as an example, the solid angle and the position of the source within the field of view are incorporated into the evaluation equation as follows [75,92]:

$$\text{UGR} = 8\log_{10}\left[\frac{0.25}{L_b}\sum_{i=1}^{n}\frac{L_i^2\omega_i}{p_i^2}\right] \tag{A2}$$

where L_b is the background luminance, L_i is the luminance of the ith glare source, ω_i is its solid angle, p_i is its position index within the field of view, and n is the number of glare sources. The angular relationships illustrated in Figure 4b are used to describe the source position within the field of view; the position index is not equivalent to any single angle shown in the figure. Equation (A2) demonstrates how these quantities are incorporated into the metric but does not imply that the original UGR discomfort categories are applicable to daytime outdoor environments.

Appendix A.2. Representative Glare Metrics and Their Original Conditions of Applicability

Table A1. Typical glare and visibility assessment metrics.

Type	Metric	Core Parameters	Result Format	Original Evaluation Basis	Typical Scenario
Discomfort glare	British Glare Index (BGI) [16,42]	Source luminance, solid angle, source position, and background luminance	Index value	Hopkinson discomfort scale	Indoor electric lighting
	Visual Comfort Probability (VCP) [93]	Aggregate glare from multiple sources	Percentage of comfortable observers	Group subjective responses	Indoor electric lighting
	CIE Glare Index (CGI) [94]	Source luminance, source position, and direct and indirect illuminance	Index value	Hopkinson discomfort scale	Indoor electric lighting
	Daylight Glare Index (DGI) [44]	Window luminance, solid angle, source position, and background luminance	Index value	Discomfort level	Indoor daylighting
	Unified Glare Rating (UGR) [92]	Luminance, solid angle, position, and background luminance of multiple sources	Index value	CIE discomfort scale	Indoor electric lighting

Table A1. *Cont.*

Type	Metric	Core Parameters	Result Format	Original Evaluation Basis	Typical Scenario
	Daylight Glare Probability (DGP) [45]	Vertical eye illuminance, source luminance, solid angle, and source position	Probability value	Participants' comfort judgments	Indoor daylighting
	Glare Rating (GR) [95]	Equivalent veiling luminance and ambient luminance	Index value	de Boer semantic scale	Outdoor electric lighting
Disability glare	Threshold Increment (TI) [96]	Veiling luminance and road-background luminance	Threshold increment percentage	Target-recognition threshold	Nighttime road lighting
Visibility	Visibility Level (VL) [97]	Actual contrast and contrast threshold	Ratio	Target-detection threshold	Road and tunnel lighting

References

1. Gordon, I. Density and the built environment. *Energy Policy* **2008**, *36*, 4652–4656. [CrossRef]
2. Pan, W.; Du, J. Effects of neighbourhood morphological characteristics on outdoor daylight and insights for sustainable urban design. *J. Asian Archit. Build. Eng.* **2022**, *21*, 342–367. [CrossRef]
3. Lee, S.; Lee, J.S. Assessing urban solar glare from glass curtain walls: Effects of street orientation and building form on sustainable design and public safety. *Sustain. Cities Soc.* **2025**, *135*, 106984. [CrossRef]
4. Ou, Y. Quantitative study of reflection of sunlight by a glass curtain wall resulting in a visual masking effect. *Appl. Opt.* **2014**, *53*, 6893–6899. [CrossRef] [PubMed]
5. Schiler, M.; Valmont, E. Microclimatic impact: Glare around the walt Disney concert hall. In Proceedings of the Solar World Congress 2005 Joint American Solar Energy Society/International Solar Energy Society Conference, Orlando, FL, USA, 6–12 August 2005; pp. 6–12.
6. Wen, J.; Ignatius, M.; Chen, E.X.; Wong, N.H. Impacts of a highly reflective stainless-steel façade on a surrounding building: A case study in Singapore. *Sustain. Cities Soc.* **2023**, *90*, 104377. [CrossRef]
7. Knoop, M.; Stefani, O.; Bueno, B.; Matusiak, B.; Hobday, R.; Wirz-Justice, A.; Martiny, K.; Kantermann, T.; Aarts, M.; Zemmouri, N.; et al. Daylight: What makes the difference? *Light. Res. Technol.* **2020**, *52*, 423–442. [CrossRef]
8. Shih, N.J.; Huang, Y.S. An analysis and simulation of curtain wall reflection glare. *Build. Environ.* **2001**, *36*, 619–626. [CrossRef]
9. Suk, J.Y.; Schiler, M.; Kensek, K. Is Exterior Glare Problematic? Investigation on Visual Discomfort Caused by Reflected Sunlight on Specular Building Facades. In Proceedings of the PLEA 2016 Conference on Passive and Low Energy Architecture. Cities, Buildings, People: Towards Regenerative Environments, Los Angeles, CA, USA, 11–13 July 2016; pp. 11–13.
10. Woo, B.; Kim, H.; Kim, J.; Baik, H.; Kim, H.K. Influence of solar glare intensity on vehicular speed variance. *J. Transp. Health* **2021**, *20*, 101020. [CrossRef]
11. Nasrollahi, N.; Shokri, E. Daylight illuminance in urban environments for visual comfort and energy performance. *Renew. Sustain. Energy Rev.* **2016**, *66*, 861–874. [CrossRef]
12. Guo, Y.; Hu, J.; Wang, R.; Qu, S.; Liu, L.; Li, Z. Study on the influence of sun glare on driving safety. *Build. Environ.* **2023**, *228*, 109902. [CrossRef]
13. Jakubiec, J.A.; Reinhart, C.F. Assessing disability glare potential of reflections from new construction: Case study analysis and recommendations for the future. *Transp. Res. Rec.* **2014**, *2449*, 114–122.
14. Ma, H.P.; Chen, P.L.; Chen, S.K.; Chen, L.H.; Linkov, V.; Pai, C.W. Population-based case–control study of the effect of sun glare on pedestrian fatalities in Taiwan. *BMJ Open* **2019**, *9*, e028350. [CrossRef] [PubMed]
15. Sun, D.; El-Basyouny, K.; Kwon, T.J. Sun glare: Network characterization and safety effects. *Transp. Res. Rec.* **2018**, *2672*, 79–92. [CrossRef]
16. Hopkinson, R.G. Evaluation of glare. *Illum. Eng.* **1957**, *52*, 305–316.
17. Sawicki, D.; Wolska, A. Glare at outdoor workplaces—An underestimated factor of occupational risk. *Energies* **2022**, *15*, 472. [CrossRef]
18. Yi, J.; Tian, Z.; Rüdisser, D.; Geisler-Moroder, D.; Zhao, Y.; Hauer, M.; Weiss, T.; Luo, T.; Zhang, B. A review of reflected sunlight from buildings: Problems and challenges. *Sustain. Cities Soc.* **2024**, *117*, 105943. [CrossRef]
19. Lee, J.; Kim, H.; Lim, E.; Shin, M.; Suk, J.Y. Reflected solar glare from building facades: A critical review of assessment methodologies. *Build. Environ.* **2026**, *287*, 113902. [CrossRef]
20. Snyder, H. Literature review as a research methodology: An overview and guidelines. *J. Bus. Res.* **2019**, *104*, 333–339. [CrossRef]

21. Hess, D.; Bucher, C. Characterisation of the glare properties of photovoltaic modules and PV systems using a photographic camera. In Proceedings of the 39th PV-Symposium, Bad Staffelstein, Germany, 27–29 February 2024.
22. Levinson, R.; Akbari, H. Effects of composition and exposure on the solar reflectance of Portland cement concrete. *Cem. Concr. Res.* **2002**, *32*, 1679–1698. [CrossRef]
23. Qin, Y.; Zhao, Y.; Chen, X.; Wang, L.; Li, F.; Bao, T. Moist curing increases the solar reflectance of concrete. *Constr. Build. Mater.* **2019**, *215*, 114–118. [CrossRef]
24. Glanville, M.J.; Kodali, P.R.; Alsailani, M.; Alsailani, M.; Neto, M. Modelling solar disability glare reflected off modern building facades. In Proceedings of the Building Simulation Applications BSA 2024, Bolzano, Italy, 26–28 June 2024; pp. 49–56. [CrossRef] [PubMed]
25. Roos, A.; Karlsson, B. Stainless steel solar mirrors—A material feasibility study. *Sol. Energy Mater.* **1989**, *18*, 233–240. [CrossRef]
26. Speroni, A.; Mainini, A.G.; Zani, A.; Paolini, R.; Pagnacco, T.; Poli, T. Experimental assessment of the reflection of solar radiation from façades of tall buildings to the pedestrian level. *Sustainability* **2022**, *14*, 5781. [CrossRef]
27. Alleman, J.; Heitzman, M. *Quantifying Pavement Albedo*; NCAT Report 19-09; National Center for Asphalt Technology: Auburn, AL, USA, 2019.
28. Sanjuán, M.Á.; Morales, A.; Zaragoza, A. Effect of precast concrete pavement albedo on the climate change mitigation in urban areas. *Sustainability* **2021**, *13*, 11448. [CrossRef]
29. Słowik, M.; Skrzypczak, P.; Wandachowicz, K. Glare impact from photovoltaic systems on driver safety. *Sustainability* **2026**, *18*, 2541. [CrossRef]
30. Babin, M.; Thorsteinsson, S.; Jakobsen, M.L.; Spataru, S.V. Glare potential evaluation of structured PV glass based on gonioreflectometry. *IEEE J. Photovolt.* **2022**, *12*, 1314–1318. [CrossRef]
31. Li, H.; Xie, N.; Zhang, X.; Sun, L.; Harvey, J.T.; Wang, L. Investigation on mixed reflection behavior of cool pavement coating and its impact on safety of road light environment. *Engineering* **2026**, *58*, 203–220. [CrossRef]
32. Waters, C.E.; Mistrick, R.G.; Bernecker, C.A. Discomfort glare from sources of nonuniform luminance. *J. Illum. Eng. Soc.* **1995**, *24*, 73–85. [CrossRef]
33. Suk, J.Y. Absolute Glare and Relative Glare Factors: Predicting and Quantifying Levels of Interior Glare and Exterior Glare Caused by Sunlight and Daylight. Ph.D. Thesis, University of Southern California, Los Angeles, CA, USA, 2014.
34. Kim, W.; Ahn, H.T.; Kim, J.T. A first approach to discomfort glare in the presence of non-uniform luminance. *Build. Environ.* **2008**, *43*, 1953–1960. [CrossRef]
35. Brzezicki, M. The influence of reflected solar glare caused by the glass cladding of a building: Application of caustic curve analysis. *Comput.-Aided Civ. Infrastruct. Eng.* **2012**, *27*, 347–357. [CrossRef]
36. Chatzipoulka, C.; Compagnon, R.; Nikolopoulou, M. Urban geometry and solar availability on façades and ground of real urban forms: Using London as a case study. *Sol. Energy* **2016**, *138*, 53–66. [CrossRef]
37. Yang, X.; Grobe, L.; Wittkopf, S. Simulation of reflected daylight from building envelopes. In Proceedings of the Building Simulation 2013: 13th Conference of the International Building Performance Simulation Association, Chambéry, France, 25–28 August 2013; pp. 1054–1061.
38. Li, X.; Cai, B.Y.; Qiu, W.; Zhao, J.; Ratti, C. A novel method for predicting and mapping the occurrence of sun glare using Google Street View. *Transp. Res. Part C Emerg. Technol.* **2019**, *106*, 132–144. [CrossRef]
39. Zhu, H.; Gu, Z. A method of estimating the spatiotemporal distribution of reflected sunlight from glass curtain walls in high-rise business districts using street-view panoramas. *Sustain. Cities Soc.* **2022**, *79*, 103671. [CrossRef]
40. Hopkinson, R.G. Discomfort glare in lighted streets. *Trans. Illum. Eng. Soc.* **1940**, *5*, 1–32. [CrossRef]
41. Luckiesh, M. Brightness in Visual Field at Borderline between Comfort and Discomfort (BCD). *Illum. Eng.* **1949**, *44*, 650–670. [PubMed]
42. Petherbridge, P.; Hopkinson, R.G. Discomfort glare and the lighting of buildings. *Trans. Illum. Eng. Soc.* **1950**, *15*, 39–79. [CrossRef]
43. de Boer, J.B.; Schreuder, D.A. Glare as a criterion for quality in street lighting. *Trans. Illum. Eng. Soc.* **1967**, *32*, 117–135. [CrossRef]
44. Hopkinson, R.G. Glare from daylighting in buildings. *Appl. Ergon.* **1972**, *3*, 206–215. [CrossRef] [PubMed]
45. Wienold, J.; Christoffersen, J. Evaluation methods and development of a new glare prediction model for daylight environments with the use of CCD cameras. *Energy Build.* **2006**, *38*, 743–757. [CrossRef]
46. Girard, J.; Villa, C.; Brémond, R. Discomfort glare from several sources: A formula for outdoor lighting. *LEUKOS* **2021**, *17*, 108–124. [CrossRef]
47. Xia, L.; Tu, Y.; Liu, L.; Wang, Y.; Peng, S.; Knoop, M.; Heynderickx, I. A study on overhead glare in office lighting conditions. *J. Soc. Inf. Disp.* **2011**, *19*, 888–898. [CrossRef]
48. Geisler-Moroder, D.; Knoflach, C. Critical review of the daylight glare probability and proposal for modification for improved evaluation of small glare sources. *Light. Res. Technol.* **2025**, *57*, 604–631. [CrossRef]
49. Kong, G.; Wang, L.; Chen, P.; Wang, S.; Ma, F. Morphological and Position Factors of Vertical Surface Light Source Affecting Discomfort Glare Perception. *Buildings* **2024**, *14*, 1227. [CrossRef]

50. Al-Sallal, K.A. Easing high brightness and contrast glare problems in universal space design studios in the UAE: Real models testing. *Renew. Energy* **2006**, *31*, 617–630. [CrossRef]
51. *CIE S 017/E:2020*; ILV: International Lighting Vocabulary. International Commission on Illumination: Vienna, Austria, 2020. [CrossRef]
52. Vos, J.J. On the cause of disability glare and its dependence on glare angle, age and ocular pigmentation. *Clin. Exp. Optom.* **2003**, *86*, 363–370. [CrossRef] [PubMed]
53. Van Den Berg, T. On the relation between glare and straylight. *Doc. Ophthalmol.* **1991**, *78*, 177–181. [CrossRef] [PubMed]
54. Schumann, J.; Flannagan, M.J.; Sivak, M.; Traube, E.C. Daytime veiling glare and driver visual performance: Influence of windshield rake angle and dashboard reflectance. *J. Saf. Res.* **1997**, *28*, 133–146. [CrossRef]
55. Gray, R.; Regan, D. Glare susceptibility test results correlate with temporal safety margin when executing turns across approaching vehicles in simulated low-sun conditions. *Ophthalmic Physiol. Opt.* **2007**, *27*, 440–450. [CrossRef] [PubMed]
56. Li, H.; Wang, J.; Zhai, H.; Hao, Y.; Chen, Y. Assessment of highway available sight distances under disability glare using a field-of-view model and traffic-signboard recognition. *IET Intell. Transp. Syst.* **2026**, *20*, e70158. [CrossRef]
57. Ishak, N.M.; Hien, W.N.; Jenatabadi, H.S.; Zawawi, E.M.A. Effect of reflective building façade on pedestrian visual comfort. In Proceedings of the 4th International Conference on Research Methodology for Built Environment and Engineering, Bangkok, Thailand, 24–25 April 2019.
58. Ishak, N.M.; Jenatabadi, H.S.; Mustafa, S.N.A.M.; Abdullah, J. The impact of building façade reflectivity on pedestrian visual comfort with the application of Bayesian structural equation modeling. *Eng. J.* **2021**, *25*, 211–223. [CrossRef]
59. Joslyn, P.; Abdelwahab, S. Reflective facades' impacts on visual perception and psychological responses. *Architecture* **2025**, *5*, 66. [CrossRef]
60. Suk, J.Y.; Schiler, M.; Kensek, K. Reflectivity and specularity of building envelopes: How materiality in architecture affects human visual comfort. *Archit. Sci. Rev.* **2017**, *60*, 256–265. [CrossRef]
61. Ayres, T.J.; Kelkar, R.; Woodruff, W.H. Driver adjustment to solar glare. In *Proceedings of the Human Factors and Ergonomics Society Annual Meeting*; SAGE Publications: Los Angeles, CA, USA, 2004; Volume 48, pp. 2221–2225. [CrossRef]
62. Mitra, S. Sun glare and road safety: An empirical investigation of intersection crashes. *Saf. Sci.* **2014**, *70*, 246–254. [CrossRef]
63. Liu, X.; Dong, W.; Li, T.; Chen, Y.; Li, G.; Zhao, X. Impact of freeway slope photovoltaic panels on drivers: A study based on driving simulator. *Sol. Energy* **2024**, *274*, 112601. [CrossRef]
64. Jurado-Piña, R.; Pardillo-Mayora, J.M. Methodology to predict driver vision impairment situations caused by sun glare. *Transp. Res. Rec.* **2009**, *2120*, 12–17. [CrossRef]
65. Shih, N.J.; Huang, Y.S. A study of reflection glare in Taipei. *Build. Res. Inf.* **2001**, *29*, 30–39. [CrossRef]
66. Wong, J.S.J. A comprehensive ray tracing study on the impact of solar reflections from glass curtain walls. *Environ. Monit. Assess.* **2016**, *188*, 16. [CrossRef] [PubMed]
67. Wang, J.; Wei, M.; Ruan, X. Comparison of daylight simulation methods for reflected sunlight from curtain walls. In *Proceedings of Building Simulation*; Tsinghua University Press: Beijing, China, 2021; Volume 14, pp. 549–564. [CrossRef]
68. Moereke, J.; Borowski, P.; Grünsteidl, S.; Palm, J.; Sapkota, S.B.; Dalibor, T. Light reflection analysis of pv modules: Comparison to building facades and assessing the possibility of glare. In Proceedings of the 8th World Conference of Photovoltaic Energy Conversion, Milan, Italy, 26–30 September 2022; pp. 1050–1056.
69. González-Collazo, S.M.; del Río-Barral, P.; Balado, J.; González, E. Detection of direct sun glare on drivers from point clouds. *Remote Sens.* **2022**, *14*, 1456. [CrossRef]
70. González-Collazo, S.M.; Solla, M.; González, E.; Rodríguez-Somoza, J.L.; Balado, J. Optimizing bus stop environments: Analysis of sun glare reduction with green elements in MLS and GPR data. *ISPRS Ann. Photogramm. Remote Sens. Spat. Inf. Sci.* **2024**, *X-4/W5-2024*, 187–194. [CrossRef]
71. Cilliers, D.P.; Retief, F.P.; Roos, C.; Alberts, R.; Moolman, H.; Bond, A. Towards glint and glare impact assessment best practice. *Impact Assess. Proj. Apprais.* **2024**, *42*, 498–504. [CrossRef]
72. Castellani, B.; Gambelli, A.M.; Nicolini, A.; Rossi, F. Optic-energy and visual comfort analysis of retro-reflective building plasters. *Build. Environ.* **2020**, *174*, 106781. [CrossRef]
73. Abdelwahab, S.; Elhussainy, M.; Labib, R. The negative impact of solar reflections caused by reflective buildings' facades: Case study of the Nasher Museum in Texas. *Proc. IOP Conf. Ser. Earth Environ. Sci.* **2019**, *297*, 012048. [CrossRef]
74. Wen, J.; Ignatius, M.; Wong, N.H. A prediction model for fast evaluation of reflective glare from surrounding buildings. *Sol. Energy* **2022**, *243*, 279–299. [CrossRef]
75. Spieringhs, R.M.; Phung, T.H.; Audenaert, J.; Hanselaer, P. Exploring the Applicability of the Unified Glare Rating for an Outdoor Non-Uniform Residential Luminaire. *Sustainability* **2022**, *14*, 13199. [CrossRef]
76. Inanici, M.N. Evaluation of high dynamic range photography as a luminance data acquisition system. *Light. Res. Technol.* **2006**, *38*, 123–134. [CrossRef]

77. Wasilewski, S.; Grobe, L.O.; Wienold, J.; Andersen, M. A critical literature review of spatio-temporal simulation methods for daylight glare assessment. *SDAR J. Sustain. Des. Eng. Built Environ.* **2019**, *7*, 4. [CrossRef]
78. Alaqtum, T.; Engineer, A.; Moeller, C. Daylighting Glare and Design for Visual Comfort. *Technol. | Archit. + Des.* **2024**, *8*, 126–142. [CrossRef]
79. Xiao, J.; Liang, B.; Niu, J.; Qin, C. Study on the glare phenomenon and time-varying characteristics of luminance in the access zone of the east–west oriented tunnel. *Appl. Sci.* **2024**, *14*, 2147. [CrossRef]
80. Peng, R.; Zhang, J.; Han, Y. Numerical modelling and dynamic evaluation of building glass curtain wall-reflected glare pollution for road vehicle drivers. *Sustainability* **2025**, *17*, 3823. [CrossRef]
81. Seo, J.; Kim, H.; Jang, H.; Kim, J.; Hong, J.; Hong, T. Interpretable predictive model-based architectural design strategies for mitigating reflected daylight glare in urban residential buildings. *Build. Environ.* **2026**, *298*, 114621. [CrossRef]
82. Girard, J.; Villa, C.; Brémond, R. Modelling the Probability of Discomfort Due to Glare at All Levels: The Case of Outdoor Lighting. *LEUKOS* **2023**, *19*, 368–388. [CrossRef]
83. Abboushi, B.; Fotios, S.; Miller, N.J. Predicting Discomfort from Glare with Pedestrian-Scale Lighting: A Comparison of Candidate Models Using Four Independent Datasets. *Light. Res. Technol.* **2024**, *56*, 225–246. [CrossRef]
84. Abboushi, B.; Miller, N.J. What to measure and report in studies of discomfort from glare for pedestrian applications. *Light. Res. Technol.* **2024**, *56*, 250–259. [CrossRef]
85. Girard, J.; Villa, C.; Brémond, R. Discomfort Glare from a Cyclic Source in Outdoor Lighting Conditions. *LEUKOS* **2022**, *18*, 459–474. [CrossRef]
86. Vissenberg, M.C.J.M.; Perz, M.; Donners, M.; Sekulovski, D. A Generic, Visual System-Based Model for Discomfort from Glare. *Light. Res. Technol.* **2023**, *55*, 400–413. [CrossRef]
87. Geisler-Moroder, D.; Knoflach, C.; Dick, M.; Hammes, S.; Weninger, J.; Pfluger, R. Daylight Glare with the Sun in the Field of View: An Evaluation of the Daylight Glare Metric Through a Laboratory Study Under an Artificial Sky Dome and an Extensive Simulation Study. *Buildings* **2026**, *16*, 249. [CrossRef]
88. Zheng, D.; Chen, Y.; Yan, D. Effects of optical scattering in aerogel glazing system on daylight illuminance and discomfort glare. *Build. Environ.* **2025**, *286*, 113765. [CrossRef]
89. Jain, S.; Wienold, J.; Lagier, M.; Schueler, A.; Andersen, M. Perceived glare from the sun behind tinted glazing: Comparing blue vs. color-neutral tints. *Build. Environ.* **2023**, *234*, 110146. [CrossRef]
90. Zheng, D.; Chen, Y.; Peng, J. Daylighting performance and discomfort glare assessment of granular aerogel glazing system: A full-scale comparative experiment. *Build. Environ.* **2023**, *236*, 110297. [CrossRef]
91. Sorooshnia, E.; Rashidi, M.; Rahnamayiezekavat, P.; Rezaei, F.; Samali, B. Optimum external shading system for counterbalancing glare probability and daylight illuminance in Sydney's residential buildings. *Eng. Constr. Archit. Manag.* **2023**, *30*, 296–320. [CrossRef]
92. *CIE 117:1995*; Discomfort Glare in Interior Lighting. International Commission on Illumination: Vienna, Austria, 1995. [CrossRef]
93. Rea, M.S. (Ed.) *The IESNA Lighting Handbook: Reference & Application*, 9th ed.; Illuminating Engineering Society of North America: New York, NY, USA, 2000.
94. Einhorn, H.D. Discomfort glare: A formula to bridge differences. *Light. Res. Technol.* **1979**, *11*, 90–94. [CrossRef]
95. *CIE 112:1994*; Glare Evaluation System for Use Within Outdoor Sports- and Area Lighting. International Commission on Illumination: Vienna, Austria, 1994.
96. *CIE 115:2010*; Lighting of Roads for Motor and Pedestrian Traffic. International Commission on Illumination: Vienna, Austria, 2010. [CrossRef]
97. Adrian, W. Visibility of targets: Model for calculation. *Light. Res. Technol.* **1989**, *21*, 181–188. [CrossRef]

Disclaimer/Publisher's Note: The statements, opinions and data contained in all publications are solely those of the individual author(s) and contributor(s) and not of MDPI and/or the editor(s). MDPI and/or the editor(s) disclaim responsibility for any injury to people or property resulting from any ideas, methods, instructions or products referred to in the content.